Biochemical and Biophysical Research Communications 417 (2012) 67–72

Contents lists available at SciVerse ScienceDirect

Biochemical and Biophysical Research Communications

journal homepage: www.elsevier.com/locate/ybbrc

The microtubule-associated protein EB1 maintains cell polarity through activation of protein kinase C

Joseph M. Schober *, Guim Kwon, Debbie Jayne, Jeanine M. Cain

Department of Pharmaceutical Sciences, Southern Illinois University Edwardsville School of Pharmacy, Edwardsville, IL 62026-2000, USA

ARTICLE INFO

Article history:
Received 10 November 2011
Available online 19 November 2011

Keywords:
EB1
Microtubules
Actin
Protein kinase C
Polarity
Migration

ABSTRACT

The plus-ends of microtubules target the cell cortex to modulate actin protrusion dynamics and polarity, but little is known of the molecular mechanism that couples the interaction. EB1 protein associates with the plus-ends of microtubules, placing EB1 in an ideal spatial position to mediate microtubule–actin cross talk. The objective of the current study was to further understand intracellular signaling involved in EB1-dependent cell polarity and motility. B16F10 mouse melanoma cells were depleted of EB1 protein using short hair-pin RNA interference. Correlative live cell-immunofluorescence microscopy was performed to determine localization of WAVE2 and IQGAP1 to protruding versus retracting edges. EB1 knock down caused poor subcellular separation of WAVE2 and IQGAP1, and overall decreased localization. Activation of PKC corrected defects in WAVE2 and IQGAP1 localization, cell spreading and cell shape to levels observed in control cells, but did not correct defects in cell migration. Consistent with these findings, decreased PKC phosphorylation was observed in EB1 knock down cells. These findings support a model where EB1 protein links microtubules to actin protrusion and cell polarity through signaling pathways involving PKC.

1. Introduction

The MAPRE genes (*MAPRE1*, *MAPRE2* and *MAPRE3*) encode the EB1 family of microtubule-binding proteins (EB1, RP1/EB2 and EBF3/EB3) [1,2]. The EB1 protein family is evolutionarily conserved with homologs found in yeast, plants and mammals [3,4]. EB1 was initially described as a binding partner of adenomatous polyposis coli (APC) [5], a tumor suppressor factor associated with colorectal cancer [6]. The C-terminal domain of EB1 is responsible for binding the C-terminal domain of APC [7]. EB1 expression is altered in various types of tumors and is associated with malignant phenotype. Expression is increased in patient samples and cell lines derived from hepatocellular [8], esophageal [9], human gastric [10] and breast [11] carcinomas; however, EB1 is decreased in pediatric ependymomas [12]. Overexpression promotes cellular growth, activation of the beta-catenin/T-cell factor pathway, tumor formation [9,13] and activation of aurora-B kinase [14]. Interestingly, gene fusion between *MAPRE1* and *MLL* was found in a patient with acute lymphoblastic leukemia [15].

Cell migration, essential for malignant cell invasion and metastasis, requires cross-communication between the microtubule system and actin cytoskeleton. EB1 protein binds specifically to the plus-ends of microtubules [16], placing EB1 in an ideal spatial position to mediate cross-talk with actin. Our previous studies identified EB1 as essential for melanoma cell motility [17] and position EB1 as a regulator of actin dynamics [17,18]. Depletion of EB1 caused decreased lamellipodia protrusion and decreased Arp3 localization in B16F1 melanoma cells [17]. In addition, attenuated lamellipodia protrusion was accompanied by increased fascin localization at the cell cortex and decreased cell migration velocity [17]. In the current studies, we investigated the role of protein kinase C (PKC) in mediating EB1-dependent polarity and actin cytoskeleton remodeling in mouse melanoma cells.

2. Materials and methods

2.1. Cell culture and reagents

B16F10 mouse melanoma cells were purchased from American Type Culture Collection (Manassas, VA, USA) and maintained in Dulbecco's Modified Eagle Medium (DMEM) supplemented with 10% fetal bovine serum (Atlanta Biologicals, Lawrenceville, GA, USA) and antibiotics. Trypsin/EDTA solution (Mediatech, Manassas, VA, USA) was used for cell detachment. Fugene 6 transfection reagent was purchased from Roche Diagnostics. Mouse laminin, Alexa Fluor 488 and Alexa Fluor 350 conjugated to phalloidin were from Invitrogen. Phorbol 12-myristate 13-acetate (PMA) was from Acros Organics. Mouse

* Corresponding author. Address: Department of Pharmaceutical Sciences, Southern Illinois University Edwardsville School of Pharmacy, 220 University Park Drive, Edwardsville, IL 62026-2000, USA. Fax: +1 618 650 5145.
E-mail address: joschob@siue.edu (J.M. Schober).

0006-291X/$ - see front matter © 2011 Elsevier Inc. All rights reserved.
doi:10.1016/j.bbrc.2011.11.056

monoclonal anti-EB1 antibodies (clone 5) and mouse monoclonal anti-IQGAP1 antibodies were purchased from BD Transduction Laboratories. The rabbit polyclonal anti-WAVE2 and anti-phosphorylated (serine 657) PKC-alpha antibodies were from Santa Cruz Biotechnology, Inc. (Santa Cruz, CA, USA). The mouse monoclonal anti-PKC alpha antibodies were purchased through Abcam. Anti-rabbit and anti-mouse secondary antibodies conjugated to TRITC or Cy5 were purchased from Jackson Immuno Research Laboratories.

2.2. Short hair-pin RNA interference

The target sequence used for knock down of EB1 protein expression was GCCTGGACCAGCAGAGCAA (EB1 KD) and the two-nucleotide mismatch control sequence was GCCTGGACAAGCAGGGCAA (MM control). The target and MM control sequences were inserted into pG-Shin vector [19]. B16F10 cells were transfected with purified plasmid using Fugene 6 reagent according to the manufacturer instructions. Experiments were performed 3 days after transfection when correlation between EB1 knock down and GFP expression was optimal.

2.3. Immunofluorescence microscopy

Glass coverslips coated with 30 μg/ml mouse laminin (Invitrogen) for 24 h at 4 °C were placed in 35 mm-diameter dishes containing DMEM with freshly thawed 10% FBS. Cells were added to the dishes and incubated for 30 min at 37 °C. For EB1 and PKC immunofluorescence, coverslips were fixed with −20 °C methanol for 5 min then 4% paraformaldehyde with 0.5% Triton X-100 in phosphate-buffered saline (PBS) for 20 min at 22 °C. For IQGAP1 and WAVE2 immunofluorescence, and for phalloidin staining, coverslips were fixed in cytoskeleton-stabilizing buffer (80 mM PIPES, 2 mM EGTA, 3 mM $MgCl_2$, pH 6.9) with 4% paraformaldehyde and 0.5% Triton X-100 for 30 min at 22 °C. Coverslips were washed in PBS, blocked with 2% bovine serum albumin and incubated with primary antibodies for 20 min at 37 °C. Coverslips were incubated with secondary antibodies and mounted onto glass slides using Aqua Poly/Mount (Polysciences, Warrington, PA, USA). Images were acquired using a Leica DMIRE2 HC inverted epifluorescence microscope fitted with a 16-bit grayscale CCD camera. Roundness index, cell area and linescan intensity were measured using Metamorph software as described previously [17]. For the live cell-immunofluorescence correlative microscopy studies, etched coverslips (Bellco Glass, Vineland, NJ, USA) were coated with 30 μg/ml laminin for 20 h at 4 °C. The coverslips were placed into Bioptechs Delta T dishes (Butler, PA, USA) containing DMEM with freshly thawed 10% FBS. After incubation for 30 min, images were acquired using a 40× phase objective at 7-s intervals for approximately 2 min followed by immediate fixation in cytoskeletal-stabilizing buffer with 4% paraformaldehyde and 0.5% Triton X-100.

2.4. Cell motility

Bioptechs Delta T dishes were coated with 25 μg/ml mouse laminin for 25 h at 4 °C. Approximately 48 h post-transfection with the EB1 knock down plasmid, cells were trypsinized and re-seeded into the laminin-coated Delta T dishes. Cells were incubated for 30 min at 37 °C prior to initiating the experiment. Phase contrast images were acquired with a 5× objective every 20 min for approximately 18 h. During the experiment, the chamber was maintained at 37 °C using the Delta T heated-lid controller system (Bioptechs) and infused with humidified, 5% CO_2–air mixture. Green fluorescence images were acquired at the beginning and end of each experiment to monitor movement of EB1 knock down cells. To analyze the data, a video of cell movement over 18 h was constructed. Individual cell positions centered on the nucleus were tracked frame-by-frame using Metamorph software. Threshold for nucleus displacement was 1.7 μm. Distance travelled, distance from origin and *x* and *y* coordinates were obtained for each frame. Average velocity was calculated from distance and time variables as described [17].

3. Results

3.1. Knock down of EB1 protein disrupts localization of WAVE and IQGAP

In our previous study we performed short hair-pin RNA interference (shRNAi) to knock down EB1 protein in the B16F1 mouse melanoma cell line. In the current study we used B16F10 cells because of their higher transfection efficiency (our unpublished observations). The plasmid encodes a short hair-pin sequence specific for EB1 knock down and a sequence for green fluorescence protein (GFP) expression. Transfected cells co-express the short-hair-pin with GFP thereby allowing identification of EB1 knock down cells [17,19]. A two-nucleotide mismatch sequence and non-transfected cells serve as controls. We achieved 87.5% knock down efficiency of EB1 protein in GFP-positive B16F10 cells as assessed by quantitative immunofluorescence (Supplementary Fig. 1 KD). The two-nucleotide mismatch control plasmid had no effect on EB1 protein fluorescence (Supplementary Fig. 1 MM). These results demonstrate achievement of high efficiency EB1 protein knock down in individual B16F10 mouse melanoma cells using a shRNAi plasmid.

In previous studies, knock down of EB1 protein enhanced fascin immunofluorescence and decreased Arp 2/3 immunofluorescence [17], markers of filopodia and lamellipodia, respectively [20,21]. In the current study, we examined immunofluorescence of two actin signaling molecules, IQGAP1 and WAVE2. Using correlative live cell-immunofluorescence microscopy we examined IQGAP1 and WAVE2 localization to retracting versus protruding edges in normal B16F10 cells. Cells were plated onto laminin for 30 min, imaged for a period of 112 s using phase contrast microscopy, fixed, and then stained for actin, IQGAP and WAVE. Protruding and retracting edges were identified using kymograph analysis (Fig. 1A). WAVE concentrated in protruding edges, while IQGAP concentrated in retracting edges (Fig. 1B). Thus, in normal polarized B16F10 cells, WAVE and IQGAP localize to separate regions of the actin cytoskeleton serving as markers for protruding and retracting cell edges, respectively. We next evaluated WAVE and IQGAP distribution in EB1 knock down cells using immunofluorescence (Fig. 2). In non-transfected (NT) and two-nucleotide mismatch (MM) controls, integrated WAVE intensity in protruding (*P*) edges was more than twice the intensity found in retracting (*R*) edges; whereas, integrated IQGAP intensity in retracting (*R*) edges was more that three-times the intensity found in protruding (*P*) edges (Fig. 2). Because in our previous studies we observed EB1 knock down cells undergo short alternating phases of protrusion and retraction, we labeled fluorescence intensity in EB1 KD cells as *PR* (Fig. 2). By contrast, separation of WAVE from IQGAP in the actin cytoskeleton in EB1 KD cells was poor and integrated intensity was altered. WAVE intensity in edges of EB1 KD cells was less than protruding edges in control cells, but more than retracting edges in control cells. IQGAP intensity in edges of EB1 KD cells was less than in retracting edges of control cells, but more than protruding edges of control cells (Fig. 2 graph).

3.2. Activation of PKC in EB1 knock down cells corrects WAVE and IQGAP localization, and defects in cell spreading and shape

We previously reported knock down of EB1 protein causes decreased cell spreading and loss of polarized cell shape [17]. We

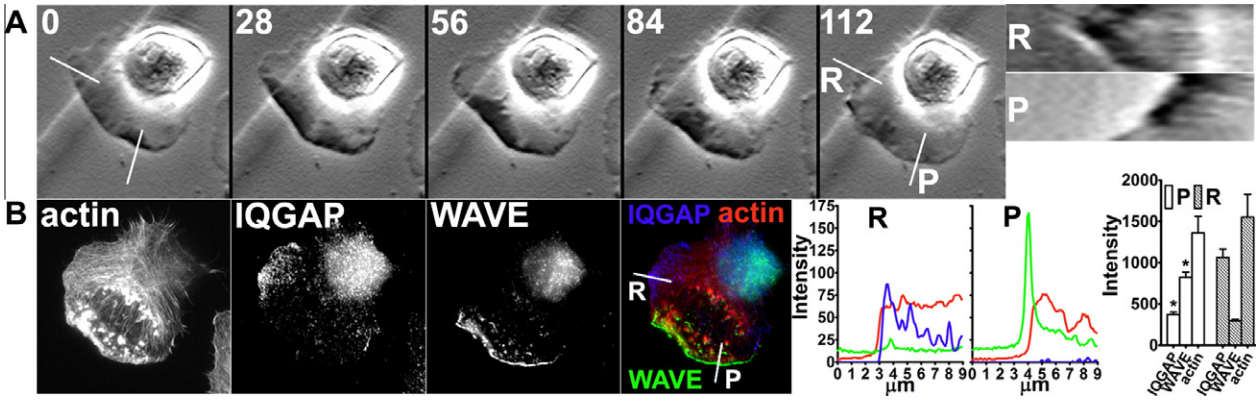

Fig. 1. IQGAP and WAVE are markers of retracting and protruding cells edges, respectively. (A) B16F10 cells were placed on laminin for 30 min then phase images were acquired at the indicated times (0–112 s). Kymographs, represented by the 14 μm-lines, identify retracting (*R*) and protruding (*P*) cell edges. (B) Cells were immediately fixed after 112 s and stained for actin, IQGAP1 and WAVE2. Fluorescence intensity profiles of actin (red), IQGAP1 (blue) and WAVE2 (green) at retracting and protruding edges (identified in A) are plotted. Integrated intensity bar graph represents 12 cells (error bars: SEM). $^{*}p < 0.01$ versus IQGAP or WAVE in retracting (*R*) edges. (For interpretation of the references to color in this figure legend, the reader is referred to the web version of this article.)

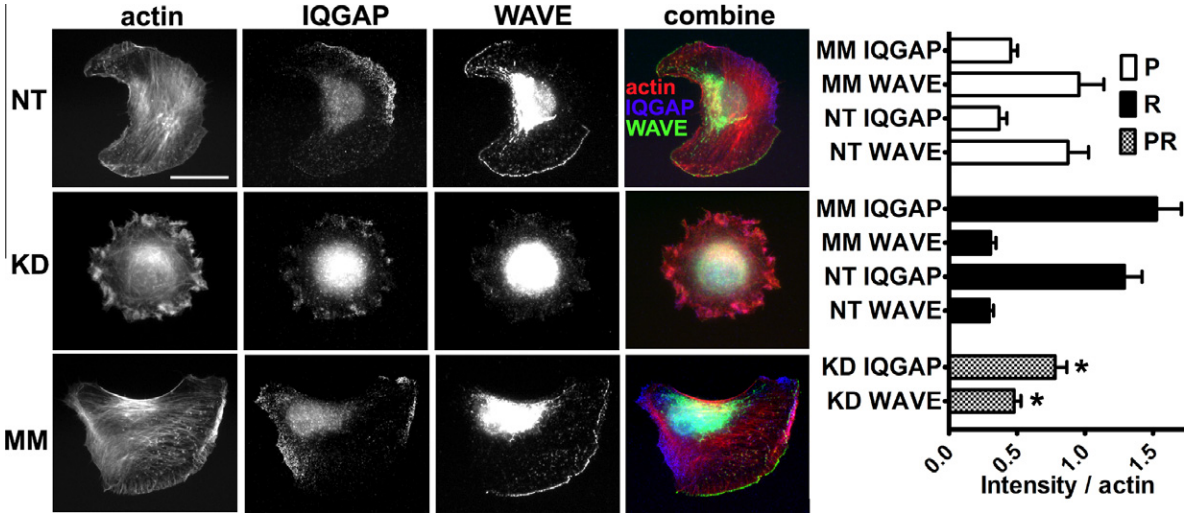

Fig. 2. EB1 knock down disrupts IQGAP and WAVE localization. B16F10 cells were plated onto laminin for 30 min, fixed and stained with IQGAP1 or WAVE2 antibodies, and Alexa Fluor 350–phalloidin. Individual actin, WAVE, IQGAP and combined images are shown for representative non-transfected control cells (NT), EB1 knock down cells (KD) and mismatch control cells (MM). Graph is plot of integrated IQGAP or WAVE intensity over actin intensity in protruding (*P*) or retracting (*R*) edges in NT and MM control cells, or edges in EB1 knock down cells (*PR*). Error bars: SEM for 12–15 cells; scale bar = 20 μm. $^{*}p < 0.05$ versus IQGAP or WAVE in both retracting and protruding edges in MM and NT control cells.

examined whether activation of protein kinase C (PKC) rescues defects in cell spreading, shape and actin signaling molecule distribution. B16F10 cells were plated onto laminin without or with 100 nM PMA for 30 min, fixed and then stained for actin, IQGAP and WAVE. Consistent with our previous results using B16F1 cells, knock down of EB1in B16F10 cells causes decreased cell spreading and increased roundness index compared to nontransfected (NT) and mismatch (MM) control cells (Fig. 3, 0 nM PMA). Activation of PKC isozymes with PMA increased cell spreading in EB1 knock down cells equal to control cells with PMA (Fig. 3, top graph). However, 100 nM PMA rescued roundness index in EB1 knock down cells to levels equal to control cells without PMA, but not with 100 nM PMA (Fig. 3, bottom graph). Furthermore, proper localization of WAVE and IQGAP was restored in the presence of 100 nM PMA. These results suggest PKC activity is decreased in EB1 knock cells causing defects in cell polarity and localization of actin signaling molecules.

3.3. EB1 knock down cells have decreased PKC alpha phosphorylation

Activation of protein kinase C (PKC) alpha is known to regulate cell migration and motility through effects on actin cytoskeleton remodeling [22]. We next determined if EB1 knock down cells have altered PKC activity through immunofluorescence measurements of total and phosphorylated PKC alpha. EB1 knock down or control cells were plated onto laminin for 30 min, fixed and stained with antibodies specific for PKC alpha and PKC alpha phosphorylated at serine 657 [23], an indicator of enzyme activity [24]. Linescan intensity analysis was performed on the cell edge in the combined images (Fig. 4). In nontransfected (NT) and nucleotide mismatch (MM) control cells without PMA, an intense peak of phosphorylated PKC alpha localized 1–2 μm from the cell edge (Fig. 4B). By contrast, intensity scans in EB1 KD cells without PMA show a gradual PKC increase from the cell edge, and less overall phosphorylation (Fig. 4B and C). Importantly, addition of 100 nM PMA

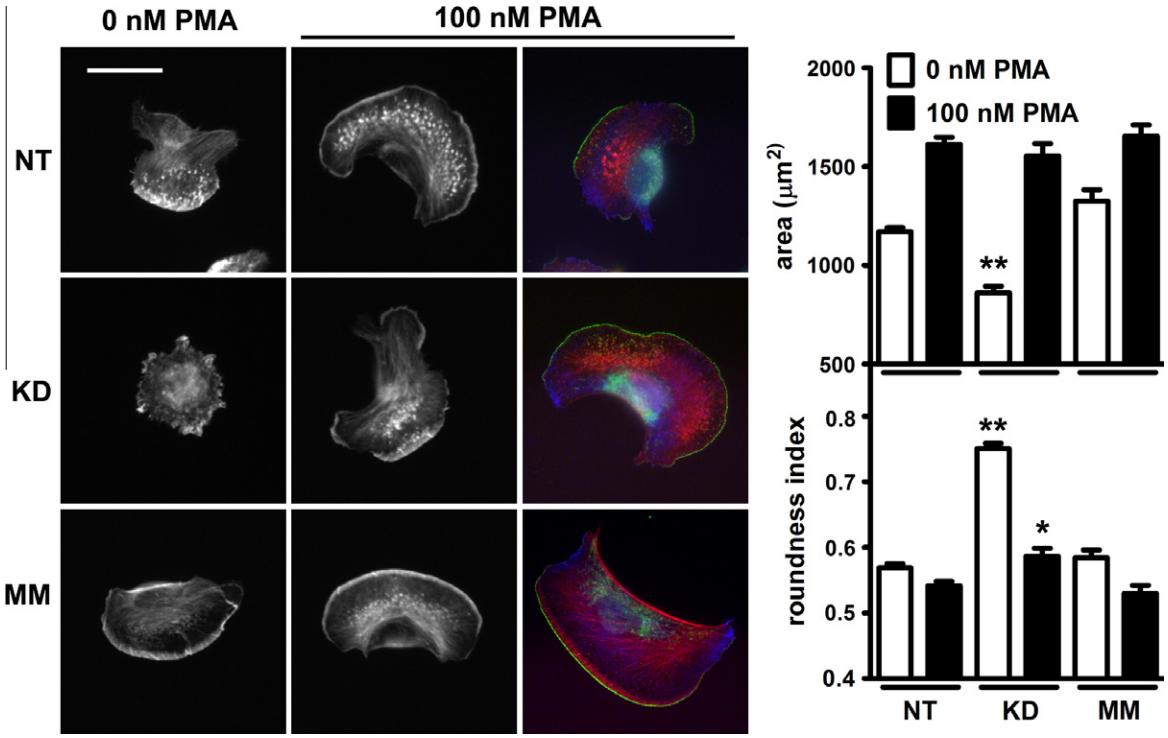

Fig. 3. Polarity defects in EB1 knockdown cells are corrected by activation with phorbol 12-myristate 13-acetate (PMA). Nontransfected (NT), EB1 knock down (KD) or mismatch control (MM) cells were plated onto laminin without or with 100 nM PMA. Cells were fixed and stained for actin (red), IQGAP1 (blue), and WAVE2 (green). Cell area and roundness index were measured (error bars = SEM; 27–32 cells/bar). Scale bar: 30 μm. $^{**}p < 0.0001$ versus KD cells with 100 nM PMA. $^{*}p < 0.002$ versus NT and MM cells with 100 nM PMA. (For interpretation of the references to color in this figure legend, the reader is referred to the web version of this article.)

increased phosphorylation in EB1 KD cells to levels equal to NT and MM control cells (Fig. 4B and C). These results indicate EB1 is required for normal localization and phosphorylation of PKC alpha.

3.4. PKC activation increases migration of normal cells, but not EB1 knock down cells

We previously reported EB1 knock down causes decreased actin protrusion at the cell edge and decreased translocation velocity [17]. We next examined if PMA rescues the defects in 2-dimensional cell motility on laminin. We measured cell velocity over 18 h and final cell distance from origin after 18 h as described previously [17]. The presence of 50 nM PMA increased both cell velocity and distance from origin of non-transfected (NT) cells (Supplementary Fig. 2); however, PMA did not increase cell velocity or distance from origin of EB1 knock down (KD) cells (Supplementary Fig. 2). These results indicate PMA-induced increase in cell migration requires EB1 protein.

4. Discussion

In our previous studies we observed polarity and motility defects in mouse melanoma cells devoid of EB1 protein. Depletion of EB1 disrupts actin dynamics through increased filopodia production and decreased lamellipodia protrusion resulting in decreased cell body migration [17]. The effect of EB1 knock down on cell migration is likely the result of inability of cells to spatially regulate intracellular signaling events needed for polarization. In our current studies, we examined the signaling mechanisms by which EB1 regulates cell polarity and motility. In polarized B16F10 cells, WAVE localizes to protruding edges while IQGAP concentrates to areas of cell retraction. EB1 knock down disrupted proper WAVE and IQGAP localization resulting in poor subcellular separation of these two actin signaling molecules which is important in motility [25,26]. Thus, poor subcellular localization of WAVE and IQGAP may explain the brief alternating periods of actin protrusion and retraction observed in EB1 knock down cells [17] as opposed to sustained protrusion coordinated with retraction in normal cells [27].

Activation of cells with PMA corrected cell spreading and shape defects, and restored proper localization of WAVE and IQGAP suggesting PKC isozymes may be involved in EB1-dependent cell polarity. Indeed, phosphorylation of PKC alpha in the cell periphery is decreased in EB1 knock down cells. Importantly, activation of cells with PMA restored PKC alpha phosphorylation to levels equal to control cells. Although PMA corrected polarity defects in EB1 knock down cells and enhanced motility of normal cells, PMA did not correct the migration defect in EB1 knock down cells. These results raise the possibility that EB1 regulates cell polarity and migration through different signaling pathways. Activation of protein kinase C isoforms is known to promote cell motility through several pathways [28–31]. Our results suggest EB1 may interact with protein kinase C signaling in a bidirectional manner. EB1 may act through PKC to maintain characteristics related to polarity including cell shape and distribution of actin signaling proteins. For example, fascin bundling activity on actin filaments is controlled by PKC phosphorylation [32]. EB1 may regulate fascin activity through PKC. Low PKC alpha activity in EB1 KD cells could result in less fascin phosphorylation; thereby, up-regulating actin bundling activity of fascin [32], consistent with hyperfilopodia formation we observed previously [17]. Also through PKC, EB1 may act to properly localize actin signaling molecules, Arp2/3, WAVE and IQGAP thereby promoting cell polarity and actin protrusion. Once polarity is established, EB1 is required for normal migration through a potentially different mechanism. During cell migration, PKC may act through EB1 because PMA enhanced the migration

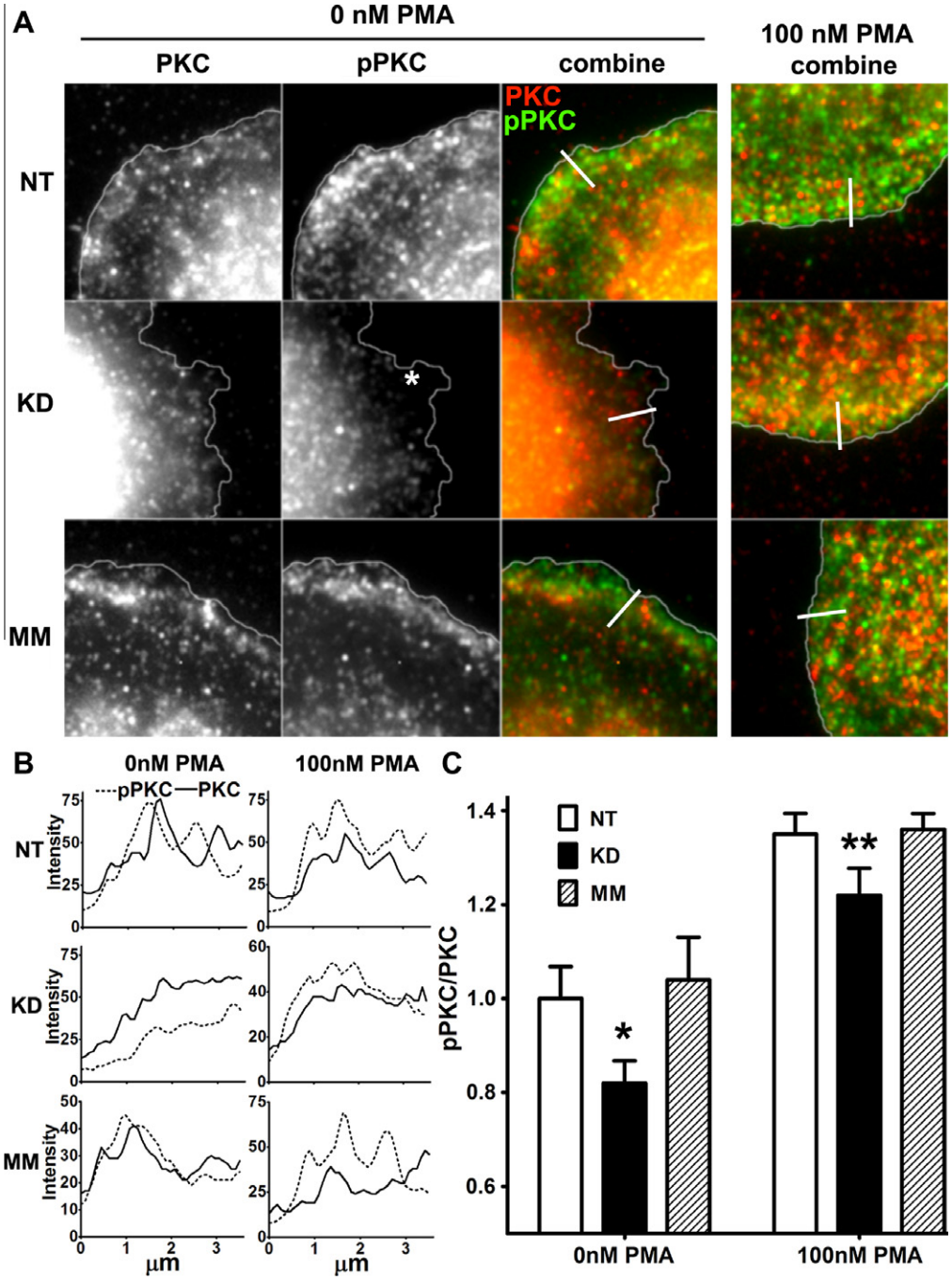

Fig. 4. Phosphorylation of PKC is decreased in EB1 knock down cells. Nontransfected (NT), EB1 knock down (KD) or mismatch control (MM) cells were plated onto laminin for 30 min. Samples were fixed in −20 °C methanol and then 4% paraformaldehyde with 0.5% Triton X-100. Cells were stained with anti-PKC alpha mouse monoclonal antibodies and anti-phosphorylated PKC (pPKC) alpha rabbit polyclonal antibodies. (A) Individual and combined images of PKC (red) and pPKC (green) in cell edges without and with 100 nM PMA. Asterisk marks decreased pPKC staining in the edge of a representative EB1 knock down cell. Lines in combined images mark positions of pPKC and PKC intensity plots shown in (B). Cell edges were traced to enhance image clarity. (B) 3.6 μm-linescans of immunofluorescence intensity over cell edges in the combined images shown in (A). (C) Integrated intensities expressed as pPKC/PKC ratios normalized to NT cells without PMA (each bar $n = 25–32$ cells). $^{*}p < 0.035$ versus 0 nM PMA NT and MM cells. $^{**}p < 0.0001$ versus 0 nM PMA KD cells. (For interpretation of the references to color in this figure legend, the reader is referred to the web version of this article.)

of normal cells, but not EB1 knock down cells. Thus, our studies taken together support a model where EB1 and PKC may interact in a bidirectional manner to establish cell polarity and maintain productive cell body migration.

Acknowledgments

This work was supported by Grants from National Institute of General Medical Sciences (J.M.S. R15GM093288), American Association of Colleges of Pharmacy and Southern Illinois University Edwardsville.

Appendix A. Supplementary data

Supplementary data associated with this article can be found, in the online version, at doi:10.1016/j.bbrc.2011.11.056.

References

[1] J.P. Juwana, P. Henderikx, A. Mischo, A. Wadle, N. Fadle, K. Gerlach, J.W. Arends, H. Hoogenboom, M. Pfreundschuh, C. Renner, EB/RP gene family encodes tubulin binding proteins, Int. J. Cancer 81 (1999) 275–284.

[2] L.K. Su, Y. Qi, Characterization of human MAPRE genes and their proteins, Genomics 71 (2001) 142–149.

[3] J.S. Tirnauer, B.E. Bierer, EB1 proteins regulate microtubule dynamics, cell polarity, and chromosome stability, J. Cell Biol. 149 (2000) 761–766.

[4] J. Chan, G.M. Calder, J.H. Doonan, C.W. Lloyd, EB1 reveals mobile microtubule nucleation sites in Arabidopsis, Nat. Cell Biol. 5 (2003) 967–971.

[5] L.K. Su, M. Burrell, D.E. Hill, J. Gyuris, R. Brent, R. Wiltshire, J. Trent, B. Vogelstein, K.W. Kinzler, APC binds to the novel protein EB1, Cancer Res. 55 (1995) 2972–2977.

[6] R. Fodde, The APC gene in colorectal cancer, Eur. J. Cancer 38 (2002) 867–871.

[7] S. Honnappa, C.M. John, D. Kostrewa, F.K. Winkler, M.O. Steinmetz, Structural insights into the EB1–APC interaction, EMBO J. 24 (2005) 261–269.

[8] K. Fujii, T. Kondo, H. Yokoo, T. Yamada, K. Iwatsuki, S. Hirohashi, Proteomic study of human hepatocellular carcinoma using two-dimensional difference gel electrophoresis with saturation cysteine dye, Proteomics 5 (2005) 1411–1422.

[9] Y. Wang, X. Zhou, H. Zhu, S. Liu, C. Zhou, G. Zhang, L. Xue, N. Lu, L. Quan, J. Bai, Q. Zhan, N. Xu, Overexpression of EB1 in human esophageal squamous cell carcinoma (ESCC) may promote cellular growth by activating beta-catenin/TCF pathway, Oncogene 24 (2005) 6637–6645.

[10] R. Nishigaki, M. Osaki, M. Hiratsuka, T. Toda, K. Murakami, K.T. Jeang, H. Ito, T. Inoue, M. Oshimura, Proteomic identification of differentially-expressed genes in human gastric carcinomas, Proteomics 5 (2005) 3205–3213.

[11] X. Dong, F. Liu, L. Sun, M. Liu, D. Li, D. Su, Z. Zhu, J.T. Dong, L. Fu, J. Zhou, Oncogenic function of microtubule end-binding protein 1 in breast cancer, J. Pathol. 220 (3) (2010) 361–369.

[12] B. Suarez-Merino, M. Hubank, T. Revesz, W. Harkness, R. Hayward, D. Thompson, J.L. Darling, D.G. Thomas, T.J. Warr, Microarray analysis of pediatric ependymoma identifies a cluster of 112 candidate genes including four transcripts at 22q12.1–q13.3, Neuro-Oncol. 7 (2005) 20–31.

[13] M. Liu, S. Yang, Y. Wang, H. Zhu, S. Yan, W. Zhang, L. Quan, J. Bai, N. Xu, EB1 acts as an oncogene via activating beta-catenin/TCF pathway to promote cellular growth and inhibit apoptosis, Mol. Carcinog. 48 (2008) 212–219.

[14] L. Sun, J. Gao, X. Dong, M. Liu, D. Li, X. Shi, J.T. Dong, X. Lu, C. Liu, J. Zhou, EB1 promotes aurora-B kinase activity through blocking its inactivation by protein phosphatase 2A, Proc. Natl. Acad. Sci. U S A 105 (2008) 7153–7158.

[15] J.F. Fu, H.C. Hsu, L.Y. Shih, MLL is fused to EB1 (MAPRE1), which encodes a microtubule-associated protein, in a patient with acute lymphoblastic leukemia, Genes Chromosomes Cancer 43 (2005) 206–210.

[16] M. Piehl, U.S. Tulu, P. Wadsworth, L. Cassimeris, Centrosome maturation: measurement of microtubule nucleation throughout the cell cycle by using GFP-tagged EB1, Proc. Natl. Acad. Sci. U S A 101 (2004) 1584–1588.

[17] J.M. Schober, J.M. Cain, Y.A. Komarova, G.G. Borisy, Migration and actin protrusion in melanoma cells are regulated by EB1 protein, Cancer Lett. 284 (2009) 30–36.

[18] J.M. Schober, Y.A. Komarova, O.Y. Chaga, A. Akhmanova, G.G. Borisy, Microtubule-targeting-dependent reorganization of filopodia, J. Cell Sci. 120 (2007) 1235–1244.

[19] S. Kojima, D. Vignjevic, G.G. Borisy, Improved silencing vector co-expressing GFP and small hairpin RNA, Biotechniques 36 (2004) 74–79.

[20] D. Vignjevic, S. Kojima, Y. Aratyn, O. Danciu, T. Svitkina, G.G. Borisy, Role of fascin in filopodial protrusion, J. Cell Biol. 174 (2006) 863–875.

[21] T.M. Svitkina, G.G. Borisy, Arp2/3 complex and actin depolymerizing factor/cofilin in dendritic organization and treadmilling of actin filament array in lamellipodia, J. Cell Biol. 145 (1999) 1009–1026.

[22] C. Larsson, Protein kinase C and the regulation of the actin cytoskeleton, Cell. Signal. 18 (2006) 276–284.

[23] F. Bornancin, P.J. Parker, Phosphorylation of protein kinase C-alpha on serine 657 controls the accumulation of active enzyme and contributes to its phosphatase-resistant state, J. Biol. Chem. 272 (1997) 3544–3549.

[24] S. Gysin, R. Imber, Replacement of Ser657 of protein kinase C-alpha by alanine leads to premature down regulation after phorbol-ester-induced translocation to the membrane, Eur. J. Biochem. 240 (1996) 747–750.

[25] T. Takenawa, H. Miki, WASP and WAVE family proteins: key molecules for rapid rearrangement of cortical actin filaments and cell movement, J. Cell Sci. 114 (2001) 1801–1809.

[26] J. Noritake, T. Watanabe, K. Sato, S. Wang, K. Kaibuchi, IQGAP1: a key regulator of adhesion and migration, J. Cell Sci. 118 (2005) 2085–2092.

[27] C. Ballestrem, B. Wehrle-Haller, B. Hinz, B.A. Imhof, Actin-dependent lamellipodia formation and microtubule-dependent tail retraction control-directed cell migration, Mol. Biol. Cell 11 (2000) 2999–3012.

[28] C.H. Eng, T.M. Huckaba, G.G. Gundersen, The formin mDia regulates GSK3beta through novel PKCs to promote microtubule stabilization but not MTOC reorientation in migrating fibroblasts, Mol. Biol. Cell 17 (2006) 5004–5016.

[29] X. Chen, S.A. Rotenberg, PhosphoMARCKS drives motility of mouse melanoma cells, Cell. Signal. 22 (2010) 1097–1103.

[30] M. Parsons, J.C. Adams, Rac regulates the interaction of fascin with protein kinase C in cell migration, J. Cell Sci. 121 (2008) 2805–2813.

[31] S.J. Slater, J.L. Seiz, B.A. Stagliano, C.D. Stubbs, Interaction of protein kinase C isozymes with Rho GTPases, Biochemistry 40 (2001) 4437–4445.

[32] Y. Yamakita, S. Ono, F. Matsumura, S. Yamashiro, Phosphorylation of human fascin inhibits its actin binding and bundling activities, J. Biol. Chem. 271 (1996) 12632–12638.